10-2013

Human cytomegalovirus infection of langerhans-type dendritic cells does not require the presence of the gH/gL/UL128-131A complex and is blocked after nuclear deposition of viral genomes in immature cells

Elvin J. Lauron
Children's Hospital Oakland Research Institute
Dong Yu
Washington University School of Medicine in St. Louis
Anthony R. Fehr
Washington University School of Medicine in St. Louis
Laura Hertel
Children's Hospital Oakland Research Institute

Journal of Virology

Human Cytomegalovirus Infection of Langerhans-Type Dendritic Cells Does Not Require the Presence of the gH/gL/UL128-131A Complex and Is Blocked after Nuclear Deposition of Viral Genomes in Immature Cells

Elvin J. Lauron, Dong Yu, Anthony R. Fehr and Laura Hertel
J. Virol. **2014, 88(1):403. DOI: 10.1128/JVI.03062-13.**
Published Ahead of Print 23 October 2013.

JVI Journals.ASM.org

Human Cytomegalovirus Infection of Langerhans-Type Dendritic Cells Does Not Require the Presence of the gH/gL/UL128-131A Complex and Is Blocked after Nuclear Deposition of Viral Genomes in Immature Cells

Elvin J. Lauron,[a] Dong Yu,[b]* Anthony R. Fehr,[b]* Laura Hertel[a]

Center for Immunobiology and Vaccine Development, Children's Hospital Oakland Research Institute, Oakland, California, USA[a]; Department of Molecular Microbiology, Washington University School of Medicine, St. Louis, Missouri, USA[b]

Human cytomegalovirus (CMV) enters its host via the oral and genital mucosae. Langerhans-type dendritic cells (LC) are the most abundant innate immune cells at these sites, where they constitute a first line of defense against a variety of pathogens. We previously showed that immature LC (iLC) are remarkably resistant to CMV infection, while mature LC (mLC) are more permissive, particularly when exposed to clinical-strain-like strains of CMV, which display a pentameric complex consisting of the viral glycoproteins gH, gL, UL128, UL130, and UL131A on their envelope. This complex was recently shown to be required for the infection of immature monocyte-derived dendritic cells. We thus sought to establish if the presence of this complex is also necessary for virion penetration of LC and if defects in entry might be the source of iLC resistance to CMV. Here we report that the efficiency of LC infection is reduced, but not completely abolished, in the absence of the pentameric complex. While virion penetration and nuclear deposition of viral genomes are not impaired in iLC, the transcription of the viral immediate early genes UL122 and UL123 and of the delayed early gene UL50 is substantially lower than that in mLC. Together, these data show that the UL128, UL130, and UL131A proteins are dispensable for CMV entry into LC and that progression of the viral cycle in iLC is restricted at the step of viral gene expression.

Myeloid dendritic cells (DC) are the most potent inducers of adaptive immune responses (1, 2) and are highly abundant in skin and mucosae, where they provide a first line of defense against invading pathogens while simultaneously acquiring antigens for subsequent presentation to T and B lymphocytes (3, 4). Tissue-resident myeloid DC are conventionally considered "immature" on the basis of their large antigen uptake capacity but relatively low T-cell stimulatory ability. Activation by danger signals such as contact with pathogens or inflammatory cytokines can then trigger their maturation and migration to the draining lymph nodes, where, as mature DC, they can stimulate naive T and B cells to proliferate and differentiate into effector T cells and antibody-producing plasma cells, respectively (5). Despite playing a critical role in the regulation of immunity, DC and their myeloid precursors can themselves become means of infection with and persistence and dissemination of numerous pathogens, including human cytomegalovirus (CMV) (6).

CMV is a ubiquitous herpesvirus that can cause severe disease in immunocompromised individuals, such as solid organ and bone marrow transplant recipients, AIDS patients, and newborns (7, 8). The oral, nasal, and genital mucosae are natural routes of CMV acquisition and spread to new hosts via urine and saliva (7–9). Mucosal DC residing at these anatomical locations are among the first cell types to encounter CMV during entry and can modulate the outcome of infection by contributing to virus dissemination during their migration toward the draining lymph nodes and by stimulating the onset of adaptive immune responses against CMV. Not surprisingly, myeloid DC are major targets of CMV's immunoevasive strategies aimed at damping and delaying the proper onset of antiviral immune responses until latency is established in hematopoietic progenitor cells (6, 10, 11).

CMV reactivation from latency is also intrinsically linked to the process of $CD34^+$ and $CD14^+$ cell differentiation into DC and macrophages (12, 13), rendering tissue-resident DC an important source of newly produced infectious virus (14–18). By reseeding key tissues such as the salivary glands with reactivated virus, these DC can effectively contribute to the horizontal transmission of CMV.

Langerhans-type DC (LC) account for the totality of innate immune cells residing in the epithelial layer of the oral mucosae, while other types of myeloid DC, displaying surface markers similar to dermal DC, reside in deeper layers, including the lamina propria and submucosa (19–22). DC populations morphologically, immunohistochemically, and ultrastructurally identical to LC can be differentiated *in vitro* from $CD34^+$ hematopoietic progenitor cells (23–26), while a type of DC considered by some to be analogous to dermal $CD14^+$ DC (25–27) and by others to be inflammatory cells distinct from resident, steady-state dermal DC (28, 29) can be obtained from monocytes (monocyte-derived DC [MDDC]).

These two types of DC differ substantially in their susceptibility

Received 17 October 2013 Accepted 18 October 2013

Published ahead of print 23 October 2013

Address correspondence to Laura Hertel, lhertel@chori.org.

* Present address: Dong Yu, Novartis Vaccines and Diagnostics, Cambridge, Massachusetts, USA; Anthony R. Fehr, Department of Microbiology, University of Iowa Carver College of Medicine, Iowa City, Iowa, USA.

doi:10.1128/JVI.03062-13

to CMV infection *in vitro*. While immature LC (iLC) are remarkably resistant regardless of the virus strain (30), immature MDDC (iMDDC) are fully permissive, but exclusively to infection by clinical-strain-like strains, which possess an extended tropism compared to that of laboratory-adapted strains (31–36). Both attenuated strain AD169*var*ATCC and clinical-strain-like strain TB40/E can initiate infection in mature LC (mLC), albeit with different efficiencies (30), while the extent of permissiveness of mature MDDC remains unclear (32, 33, 35, 36).

A pentameric complex that consists of the viral proteins gH, gL, UL128, UL130, and UL131A and is displayed on the envelope of endotheliotropic but not laboratory-adapted strains was recently shown to be required for virion entry into monocytes and endothelial and epithelial cells (37–40). Strains naturally lacking the expression of a functional UL131 (e.g., AD169*var*ATCC), UL130 (e.g., Towne*var*RIT$_3$), or UL128 (e.g., Merlin) protein, as well as viruses engineered to carry mutations in these open reading frames (ORFs) (41–43), failed to initiate infection in all three cell types, indicating that each of these proteins is individually required for tropism (37, 38, 44). All three gene products were also shown to be indispensable for direct infection of iMDDC and for virion transfer from infected human umbilical vein endothelial cells to iMDDC (37, 45).

We previously showed that mLC can be productively infected with AD169*var*ATCC, a strain containing the gH/gL/gO, but not the gH/gL/UL128-131A, complex on its envelope (46, 47). We thus asked whether the pentameric complex is actually required for CMV infection of LC. We found that both iLC and mLC could be readily accessed by all of the strains tested, irrespective of the gH/gL complex combination present on their envelopes, suggesting that the UL128-131A proteins are not essential for CMV entry into LC.

Consistent with our previous findings (30), onset of productive infection in iLC remained extremely inefficient. To identify the source of this resistance, the progress of infection in iLC was compared to that in mLC. While no substantial difference was observed in the proportion of penetrated virions or in the number of viral genomes reaching the nucleus, the efficiency of UL122/UL123 and UL50 ORF transcription was severely reduced in iLC, leading to a nearly complete loss of expression of essential immediate early protein 1 (IE1) and IE2.

Together, these data show that CMV entry into iLC and mLC is not restricted to strains harboring the gH/gL/UL128-131A complex on their envelopes and that infection progress in iLC is blocked at the step of viral immediate early gene expression, with negative consequences for the efficient progression of the viral cycle.

MATERIALS AND METHODS

Cells. Human foreskin fibroblasts (HFF, a kind gift from E. S. Mocarski, Emory University, Atlanta, GA) and ARPE-19 retinal pigment epithelial cells (a gift from M. McVoy, Virginia Commonwealth University, Richmond, VA) were propagated in Dulbecco's modified Eagle medium supplemented with 10% fetal clone serum III (HyClone), 100 U/ml penicillin, 100 μg/ml streptomycin, 4 mM HEPES, and 1 mM sodium pyruvate (Gibco, Life Technologies, Grand Island, NY). CD34$^+$ hematopoietic progenitor cells were magnetically separated with the CD34 MicroBead kit (Miltenyi Biotec, Auburn, CA) from mononuclear cells obtained by Ficoll-Hypaque density gradient centrifugation of peripheral blood samples collected in the Department of Hematology, Pediatric Sickle Cell Program and Apheresis Program, Children's Hospital & Research Center Oakland, Oakland, CA. iLC populations were obtained by culturing CD34$^+$ cells at a density of 1×10^4 to 2.5×10^4 per well in 48-well tissue culture plates with serum-free X-VIVO 15 medium (Lonza/BioWhittaker, Allendale, NJ) supplemented with 1,500 IU/ml of granulocyte-macrophage colony-stimulating factor (GM-CSF, Leukine [sargramostim]; Immunex, Seattle, WA), 2.5 ng/ml of tumor necrosis factor α, 20 ng/ml of stem cell factor, 100 ng/ml of Flt3 ligand, and 0.5 ng/ml of transforming growth factor β1 (all purchased from Peprotech, Rocky Hill, NJ) for 10 days as previously described (30, 48, 49). mLC were subsequently obtained by exposing iLC to X-VIVO 15 medium containing 10% fetal bovine serum, 200 ng/ml of CD40 ligand (Immunex, Seattle, WA), 1,500 IU/ml of GM-CSF, and 250 ng/ml of lipopolysaccharide (Sigma-Aldrich, St. Louis, MO) for 2 days.

Virus strains. AD169*var*ATCC (50), originally purchased from the American Type Culture Collection (ATCC), and Towne GFP-IE2, a green fluorescent protein (GFP)-tagged derivative of Towne*var*RIT$_3$ (51), were gifts from E. S. Mocarski (Emory University, Atlanta, GA). TR-GFP, a gift from D. Yu (Washington University, St. Louis, MO), was derived from pTR*gfp*, a bacterial artificial chromosome (BAC) clone of the clinical isolate TR (52) carrying the BAC vector sequence juxtaposed to a loxP site in place of the US2-5 region (53). In TR-GFP, the missing US2-5 region in pTR*gfp* was repaired, a second loxP site was inserted to bracket the BAC vector sequence for its excision during virus reconstitution, and a GFP expression cassette was introduced for tracking of infection. This simian virus 40 promoter-driven green fluorescent protein (GFP) expression cassette was inserted into the intergenic region between US7 and US8 and in the same transcriptional orientation as these two ORFs to minimize potential interference with their expression. Reconstitution of the TR-GFP virus, containing the full-length viral genome and expressing GFP, was then done by electroporation of MRC-5 cells with 5 μg of purified pTR*gfp* BAC DNA and with 1 μg each of expression plasmids encoding pp71 and the Cre recombinase to promote the excision of the BAC vector sequence. The US17 deletion mutant virus TR*sub*US17 was derived from pTR*gfp* by replacing the 882-bp sequence encoding US17 with a 2.3-bp GalK/kanamycin cassette (A. Fehr and D. Yu, unpublished). BADrUL131-Y4 (39), a gift from M. McVoy (Virginia Commonwealth University, Richmond, VA), was derived from a variant of the AD169 BAC clone BAD*wt* (54) containing the GFP sequence, an internal ribosomal entry site, the puromycin resistance gene in lieu of the UL21.5 ORF (55), and the wild-type UL131A sequence from TR replacing the mutated original AD169 sequence (39). *Escherichia coli* bacteria harboring the BAC clones of CMV strains TB40-BAC4 (56) and TB40-BAC4 UL128ccta82-86 were gifts from C. Sinzger (University of Ulm, Ulm, Germany). UL128ccta82-86 was derived from TB40-BAC4 by replacing the nucleotide sequence encoding the charged amino acid cluster HSLTR of UL128 with the nucleotide sequence encoding the neutrally charged amino acid stretch ASLTA, yielding a mutant virus incapable of assembling the gH/gL/UL128-UL131A complex (43). Live virus was reconstituted by transfection of BAC DNA in HFF with the Polyfect Transfection reagent in accordance with the manufacturer's instructions (Qiagen). Transfected cells were maintained with regular medium changes until a 100% cytopathic effect was observed. The supernatant was then harvested and used as the inoculum for virus amplification. All strains were propagated on HFF and purified by ultracentrifugation as previously described (30). Virus titers were determined by plaque assay on HFF monolayers in 24-well tissue culture plates. Six (TB40-BAC4), four (TB40-BAC4 UL128ccta82-86), three (BADrUL131-Y4), four (AD169*var*ATCC), four (Towne GFP-IE2), four (TR-GFP), and three (TR*sub*US17) different stocks of each virus were used for the experiments described. The identity of each strain was verified by PCR amplification of viral DNA extracted from virion preparations with primers mapping to the UL128-UL131A locus, followed by bidirectional sequencing of the DNA.

Cell infection. HFF and ARPE-19 cells were plated at a density of $\sim 2 \times 10^4/\text{cm}^2$ 3 days before exposure to CMV at a multiplicity of infection (MOI) of 5 or 10 PFU/cell or to medium alone (mock). The virus

inoculum was left in contact with cells at 37°C in 5% CO_2 until the time of harvest or for only 4 h. In the latter experiments, after removal of the inoculum, cells were washed twice, treated with citrate buffer (40 mM citric acid, 10 mM KCl, 135 mM NaCl, pH 3) for 1 min (min) at room temperature (RT) to inactivate residual bound virus (57), washed again twice, and incubated in fresh medium until harvest. At the end of the differentiation (iLC) or maturation (mLC) period, LC were harvested, counted, resuspended in fresh differentiation or maturation medium again, and exposed to CMV at an MOI of 10 or 100 PFU/cell. The virus inoculum was then left in contact with the cells until the time of harvest. In selected experiments, after removal of the inoculum, cells were washed twice in medium prior to treatment with citrate buffer as described above or with 1 mg/ml of proteinase K for 1 h at 4°C to proteolytically remove cell surface virions (58–60). Cells were then washed again twice, pelleted, and stored at −80°C for subsequent analyses or incubated in fresh medium until harvest.

IFA. For immunofluorescence staining analyses (IFA), HFF and ARPE-19 cells were plated on 12-mm-diameter glass coverslips, while iLC and mLC were harvested and deposited on glass slides by centrifugation at 800 rpm for 3 min at RT with a Cytospin 4 (Thermo Shandon). Cells were fixed in 1% formaldehyde for 30 min at RT, permeabilized in 0.5% Triton X-100 for 20 min on ice, and treated with blocking buffer (40% goat serum–40% fetal bovine serum in phosphate-buffered saline [PBS]) for 30 min at RT. Samples were then incubated with mouse monoclonal antibodies against the viral IE1/IE2 proteins (1:500, MAb810; Chemicon, Temecula, CA) or against pp150 (1:400, originally from W. Britt, Birmingham, AL) for 1 h at RT in a humidified chamber, washed in blocking buffer, and incubated with Alexa Fluor 594-conjugated goat anti-mouse antibodies (1:500; Molecular Probes, Eugene, OR) for 1 h at RT. For dual staining, cells were incubated in blocking buffer containing mouse monoclonal anti-pp150 antibodies and rabbit polyclonal anti-lamin B antibodies (1:50; Santa Cruz Biotechnology, Santa Cruz, CA) for 1 h at RT, washed in blocking buffer, and incubated with Alexa Fluor 594-conjugated goat anti-mouse and Alexa Fluor 488-conjugated goat anti-rabbit antibodies (1:500; Molecular Probes, Eugene, OR) for another hour at RT. Nuclei were labeled with Hoechst 33342 (0.2 mg/ml; Molecular Probes, Eugene, OR) for 3 min at RT. Slides were mounted in 90% glycerol–10% PBS containing 2.5 g/liter of 1,4-diazabicyclo-(2,2,2)-octane (DABCO; Alfa Aesar, Pelham, NH) prior to viewing on a Nikon Eclipse E600 fluorescence microscope equipped with iVision-Mac imaging software or on a Zeiss LSM710 confocal inverted microscope equipped with Zeiss ZEN image-processing software. Processing and three-dimensional reconstructions of confocal z-stack images were conducted with the Bitplane Imaris Suite package of Scientific Volume Imaging (Hilversum, The Netherlands) and the Surpass Surfaces and the Surpass Section visualization tools.

FISH assays. Probes consisted of a mixture of 10 pSC-B plasmids (StrataClone Ultra Blunt PCR Cloning kit; Agilent Technologies, Santa Clara, CA) containing the following DNA fragments from the genome of CMV strain FIX-BAC (AC146907): nucleotides (nt) 69050 to 77680 (8,630 nt in length), 77680 to 86900 (9,220 nt), 86900 to 94700 (7,800 nt), 94400 to 102800 (8,400 nt), 136500 to 143600 (7,100 nt), 143300 to 150200 (6,900 nt), 149800 to 156800 (7,000 nt), 166400 to 173500 (7,100 nt), 173350 to 178000 (4,650 nt), and 178000 to 184700 (6,700 nt). Two micrograms of a pSC-B plasmid mixture was labeled by nick translation in the presence of 0.004 U of DNase I (New England BioLabs), 10 U of DNA polymerase I (New England BioLabs), and 10 μM ChromaTide Alexa Fluor 594-5-dUTP (Molecular Probes, Eugene, OR) at 15°C for 75 min. Labeled probes were then cleaned with the QIAquick Gel Extraction kit (Qiagen, Valencia, CA) and resuspended in fluorescence *in situ* hybridization (FISH) buffer (2× SSC [1× SSC is 0.15 M NaCl plus 0.015 M sodium citrate], 50% deionized formamide, 20% dextran sulfate).

iLC and mLC were harvested and deposited on glass slides by centrifugation as described above. Slides were then fixed in cold 95% ethanol–5% glacial acetic acid for 5 min at −20°C, rinsed once in 100% ethanol, and air dried prior to prehybridization in FISH buffer for 30 min at 37°C in a humidified slide hybridization chamber. After the addition of 5 to 10 μl of labeled probe, slides were incubated at 95°C for 2 min to denature DNA. Hybridization was then carried out in a moist hybridization chamber overnight (18 to 20 h) at 37°C. Slides were subsequently washed with 2× SSC twice for 5 min at 60°C and once for 5 min at RT, dried, and stained with Hoechst 33342 (0.2 mg/ml) for 3 min at RT. After three washes in PBS, slides were mounted in ProLong Gold Antifade Reagent (Molecular Probes, Life Technologies, Grand Island, NY) and viewed on a Zeiss LSM710 confocal inverted microscope equipped with Zeiss ZEN image-processing software.

Real-time quantitative genomic PCR and reverse transcription-PCR. Genomic DNA was extracted from infected HFF, ARPE-19 cells, iLC, and mLC with the QIAamp DNA minikit (Qiagen, Valencia, CA). mRNA was obtained from infected iLC and mLC with the μMACS mRNA isolation kit (Miltenyi Biotec, Bergisch Gladbach, Germany), treated with DNase (DNA-free kit; Invitrogen, Life Technologies, Grand Island, NY) to remove any contaminating genomic DNA, and reverse transcribed with SuperScript II reverse transcriptase (Invitrogen, Life Technologies, Grand Island, NY). Real-time quantitative PCRs were performed in triplicate with iTaq SYBR green Supermix with ROX (Bio-Rad, Hercules, CA) and an ABI7900 thermocycler (Applied Biosystems, Carlsbad, CA) with primers hybridizing to exon 2 of the viral UL122 and UL123 ORFs (forward primer, 5′-GGCCGAAGAATCTCTCAAAA-3′; reverse primer, 5′-TCGTTGCAATCCTCGGTCA-3′), to the viral UL50 ORF (forward primer, 5′-AGAATTCATGGAGATGAACAAGGTT-3′; reverse primer, 5′-ACTCGAGTCAGTCGCGGTGTGC-3′), or to the cellular albumin gene (forward primer, 5′-GCTGTCATCTCTTGTGGGCTGT-3′; reverse primer, 5′-AAACTCATGGGAGCTGCTGGTT-3′). The following cycling parameters were used: 95°C for 2 min to activate the iTaq polymerase, followed by 40 cycles of template denaturation at 95°C for 15 s, primer annealing at 51°C (UL122/123 and UL50) or 57°C (albumin) for 30 s, and product extension at 72°C for 30 s. Absolute quantifications of viral genome, viral transcript, and cellular genome amounts were obtained by using a standard curve made by serial dilutions of plasmid pON303 (61), a kind gift from E. S. Mocarski (Emory University, Atlanta, GA), of plasmid LNCX UL50-HA (62), and of a plasmid we constructed (pTOPO-albumin) that contains a portion of the albumin gene corresponding to nt 16,000 to 16,500. The number of viral genome copies per cell was then calculated as follows: number of viral genome copies per cell = number of viral DNA copies/(number of albumin DNA copies/2) (63).

RESULTS

The UL128-131A proteins are not required for CMV infection of iLC and mLC. We previously showed that CMV strain AD169*var*ATCC can infect mLC, despite lacking the gH/gL/UL128-131A complex. This suggested that the UL128-131A proteins might not be tropism determinants for this type of DC. To test this idea, iLC and mLC populations differentiated from the $CD34^+$ progenitor cells of multiple donors were exposed to CMV strains displaying different gH/gL complex combinations on their envelopes and the efficiency of infection onset was assessed by determining the percentage of cells expressing the IE1/IE2 proteins at 48 hpi. Infections of ARPE-19 epithelial cells were conducted in parallel for comparison. The strains used in this study and their gH/gL envelope complexes are listed in Table 1. Briefly, virions from the UL128mut, AD169, and Towne strains display only the gH/gL/gO trimer (43, 46, 47, 64), while TR, BAC4, and BADr particles harbor both the gH/gL/gO and gH/gL/UL128-131A entry complexes (39, 40, 65).

To directly compare the infectious properties of each strain for each cell type in an unbiased way, the following experimental conditions were implemented. First, all virus stocks were generated and titers were determined in HFF, in order to standardize the

TABLE 1 Name and envelope complex composition of the CMV strains used in this study

Full name	Name used in text	ORF(s) deleted for BAC insertion	Origin	gH gL gO	gH gL UL128 UL130 UL131A	Reference(s) for virion complex
AD169*var*ATCC	AD169	None	Plaque-purified derivative of ATCC stocks	Yes	No	46, 47, 64
Towne GFP-IE2	Towne	None	GFP-IE2-expressing derivative of Towne*var*RIT$_3$	Yes	No	64
TR-GFP	TR-GFP	None	GFP-expressing derivative of TR-BAC containing a full-length genome	Yes	Yes	65
TR*sub*US17	TR*sub*US17	None	TR-GFP derivative carrying the GalK/kanamycin cassette in lieu of the US17 ORF	Yes	Yes	65
TB40-BAC4	BAC4	US2-US6	Highly endotheliotropic BAC clone of TB40/E	Yes	Yes	40, 65, 66
TB40-BAC4 UL128ccta82-86	UL128mut	US2-US6	BAC clone of TB40/E with the HSLTR amino acid sequence of UL128 mutated to ASLTA	Yes	No	43
BADrUL131-Y4	BADr	UL21.5	BAC clone of AD169 with the UL21.5 ORF replaced with the GFP and kanamycin resistance genes and the original UL131A ORF replaced with the UL131A ORF from strain TR	Yes	Yes	38

effects of the producer cell type on the tropism and entry modes of the viral progeny (66, 67). HFF were chosen on account of their abilities to support the growth of the AD169, Towne, and UL128mut strains and to produce viral particles with a tropism broader than that of those released by endothelial cells (66).

Second, at least three different stocks of each strain were tested, in order to assess the robustness of each strain's behavior and to minimize the effect of adventitious mutations potentially arising during CMV amplification *in vitro*. As the growth of clinical-strain-like strains on HFF is associated with the relatively rapid appearance of mutations in the ORFs encoding the UL128, UL130, and UL131A proteins (68), the nucleotide sequence of the UL128-131A genomic locus of each strain was verified by PCR amplification and sequencing of virion DNA.

Third, infections were carried out in the absence of adsorption-enhancing treatments such as exposure to polyethylene glycol or centrifugation to test the natural capacity of each strain to access cells (59, 66, 69–72). Finally, viruses were left in contact with cells until the time of harvest, in order to avoid the centrifugation step required to remove the virus inoculum from LC cultures growing in suspension.

Consistent with expectations (39), BAC4 and BADr expressed the IE1/IE2 proteins in the majority of ARPE-19 cells, while AD169, Towne, and UL128mut initiated infection in less than 0.5% of the cells (Table 2). In contrast, and contrary to published data obtained with the TR strain (59), TR-GFP failed to infect cells with high efficiency, despite carrying an intact UL128-131A locus. To verify this finding, we tested the infectivity of a different TR-GFP-derived virus, TR*sub*US17, which lacks the ORF encoding US17 (D. Yu, unpublished data). Although the function of US17 is not known, this protein is not expected to be directly involved in CMV tropism. Similar to TR-GFP, TR*sub*US17 also inefficiently infected ARPE-19 cells (Table 2), indicating that the observed phenotype was not due to changes occurring during amplification of the TR-GFP strain in our experiments and suggesting that other viral determinants of tropism for epithelial cells are likely to exist in addition to the UL128-131A proteins. Mutations in the ORF(s) encoding this as-yet-unidentified factor(s) and arising within the TR-GFP genome would be maintained in the derived virus TR*sub*US17, producing identical phenotypes with respect to these strains' tropism for epithelial cells.

Consistent with our previous findings (30), mLC were overall more permissive to infection than iLC were (Fig. 1A and B). Similar to ARPE-19 cells, BAC4 and BADr were more efficient than UL128mut and AD169 at initiating infection in mLC, while TR-GFP yielded the lowest percentage of IE1/IE2$^+$ cells (Fig. 1B). As the extent of infection was highly dependent on the donor of the progenitor cells used to differentiate LC, the infectivities of strains possessing or not possessing the gH/gL/UL128-131A complex were compared in side-by-side infections of mLC derived from the same donors (Fig. 1C and D). The percentage of infected mLC observed after exposure to BAC4 was virtually identical to that detected after exposure to UL128mut in cultures derived from 3 of 11 donors and 2- to 5-fold higher in the remaining cultures (Fig. 1C), with an overall median BAC4/UL128mut ratio of 2.3 ± 1.5. Similarly, the ratio of the percentages of BADr- and AD169-infected cells was ~1 for mLC derived from two of nine donors and ranged between 1.4 and 2.6 for the rest of the cultures (Fig. 1D), with a median value of 1.8 ± 0.5.

Both TR-GFP and TR*sub*US17 did not effectively enter mLC, yielding percentages of IE1/IE2$^+$ cells 3.5-fold (TR-GFP) and

TABLE 2 Percentages of IE1/IE2$^+$ ARPE-19 cells after infection at an MOI of 10

CMV strain	Median % of IE1/IE2$^+$ ARPE-19 cells (SD)	No. of stocks tested	No. of replicate tests
BAC4	48 (5.4)	3	3
UL128mut	0.02 (0.1)	2	5
BADr	100 (0)	2	6
AD169	0.24 (0.4)	3	18
Towne	0.12 (0.4)	3	5
TR	1.81 (1.3)	4	8
TR*sub*US17	2.53 (2)	3	5

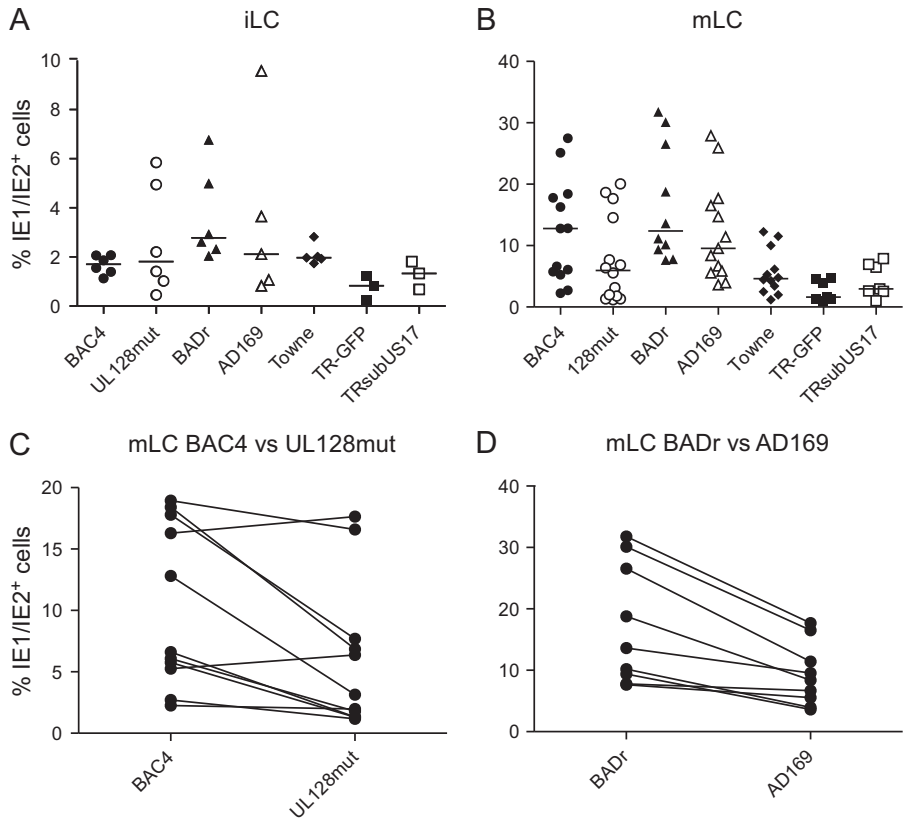

FIG 1 Efficiency of iLC and mLC infection by CMV strains carrying different entry complexes on their envelopes. (A and B) Percentages of IE1/IE2$^+$ cells after infection of iLC (A) or mLC (B) with different CMV strains at an MOI of 10 PFU/cell. Each symbol represents a separate donor of CD34$^+$ progenitor cells used to differentiate iLC and mLC populations. A horizontal bars marks the median value of each group. (C and D) Percentages of IE1/IE2$^+$ cells obtained after side-by-side infections of mLC derived from 11 (C) and 9 (D) different donors.

2-fold (TR*sub*US17) lower than those observed after infection with BAC4 (six donors). Similar to the situation in ARPE-19 cells, TR*sub*US17 was slightly more efficient than TR-GFP at initiating infection of mLC, with a median TR*sub*US17/TR-GFP ratio of 1.7 ± 0.3 (nine donors).

Aside from being more resistant to infection, iLC responses to each strain were largely similar to those of mLC, with BADr being better than AD169, TR*sub*US17 being better than TR-GFP, and BAC4 being better than both TR-GFP and TR*sub*US17 at initiating infection (Fig. 1A). In contrast to mLC, however, exposure to BAC4 or UL128mut yielded virtually identical proportions of infected cells, with a median BAC4/UL128 ratio of 0.9 ± 1.6 in parallel infections of cultures derived from six donors.

Thus, absence of the gH/gL/UL128-131A complex from the virion envelope effectively abolished viral entry into ARPE-19 cells and had essentially no impact on iLC infection but reduced the efficiency of mLC infection by approximately 2-fold. These data therefore indicate that, in contrast to epithelial cells, the presence of the UL128, UL130, and UL131A proteins is irrelevant for viral entry into iLC and is advantageous but not essential for entry into mLC. The low infectivity of TR-GFP for iLC, mLC, and ARPE-19 cells, moreover, implies that other viral proteins besides UL128, UL130, and UL131A may have a role in mediating CMV tropism for epithelial cells and LC. Finally, the small but consistent difference between the efficiencies of infection of TR-GFP and TR*sub*US17 may hint at a potential role for US17 in restraining infection onset in LC and ARPE-19 cells, identifying this protein as a potential temperance factor (73).

CMV virion entry is not blocked in iLC. The fact that no viral strain with the ability to initiate productive infection in iLC has been found hints at the presence of host defense mechanisms that cannot be overcome by any viral protein encoded by the strains tested so far.

To identify the step in the viral cycle that is blocked in iLC, the progress of viral particles was tracked by staining infected iLC and mLC for pp150, a tegument phosphoprotein that remains strongly associated with capsids during entry and has been used as a capsid marker by us and others (60, 74, 75). Cytospin preparations of iLC and mLC exposed to BAC4 at an MOI of 10 PFU/cell and harvested at 0.25, 1, 5, 20, and 30 hpi were fixed and permeabilized prior to the addition of anti-pp150 antibodies. The efficacy of permeabilization was verified by staining cells with antibodies against the nuclear envelope protein lamin B. While no signal corresponding to pp150 was observed in mock-infected, permeabilized iLC (Fig. 2A to C) or mLC (not shown), viral particles were clearly visible as bright dots (Fig. 2D and G) in infected samples. At each of the times tested, the overall abundances of viral particles appeared to be similar in infected iLC and mLC (Fig. 2, compare D and G; data not shown). To precisely quantify these data, the number of particles per cell observed in at least 200 cells from at least five different fields per time point was determined and the median number of virions per iLC versus the mLC

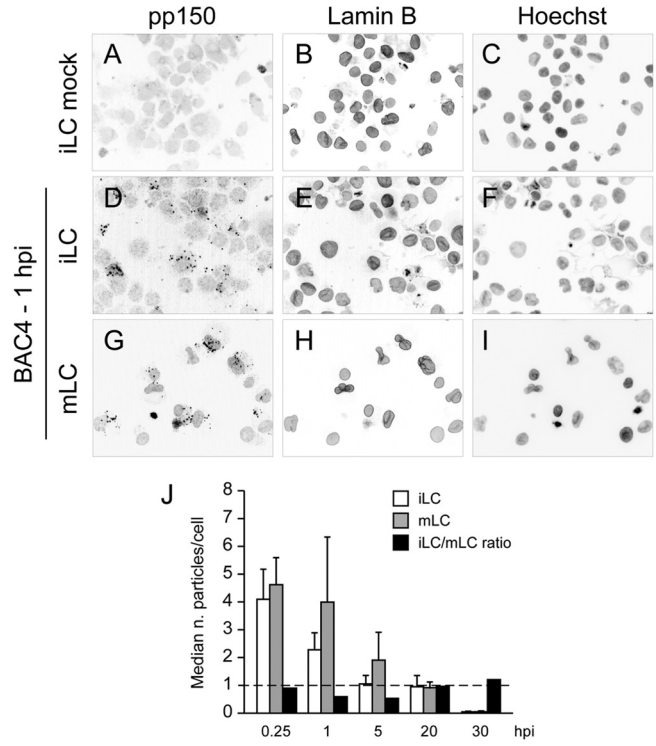

FIG 2 CMV particle density on iLC and mLC at early times postinfection. (A to I) iLC and mLC populations differentiated from the progenitor cells of a representative donor were left untreated (mock) or exposed to BAC4 at an MOI of 10 PFU/cell. Cells were harvested at 0.25, 1, 5, 20, and 30 hpi, washed once in medium, and centrifuged on glass slides. Samples were then fixed, permeabilized, and stained for pp150 (left panels) and lamin B (middle panels). Nuclei were counterstained with Hoechst 33345 (right panels). (J) Median number of viral particles per mLC or per iLC observed in 280 to 1,170 iLC found in 5 to 15 different microscopy fields and in 210 to 410 mLC found in 6 to 11 fields. Standard deviations and iLC/mLC ratios are shown. The dashed line represents an iLC/mLC ratio of 1.

ratio was calculated (Fig. 2J). At 15 min postinfection, iLC and mLC populations appeared to harbor similar numbers of particles/cell, with mean values of 4 ± 1 for iLC and 4.6 ± 1 for mLC (Fig. 2J, 0.25 hpi), indicating that the efficiencies of virion attachment and initial entry into the two cell types were highly comparable, albeit lower than expected for an MOI of 10 PFU/cell. At both 1 and 5 hpi, mLC contained approximately 40% more particles than iLC did, but by 20 hpi, these differences had waned and both cell types again contained similar number of particles. No disparity was observed at 30 hpi either, although the total amount of virions was greatly reduced from the beginning of infection, potentially because of capsid disassembly after viral genome delivery into the nucleus. Thus, while mLC appeared to contain slightly larger amounts of virions than iLC did at early times, similar number of particles were found in each cell type at later time points, suggesting that virion entry into iLC is not dramatically hindered.

As these assays did not allow us to distinguish between virions attached to the cell surface and those that had already penetrated the cell, we next treated infected cells with citrate buffer, which was expected to inactivate and detach nonpenetrating virions the cell from its surface (57, 76–78), or with proteinase K, which has been reported to proteolytically remove residual extracellular particles (58–60). Real-time quantitative PCR was then used instead of IFA to determine the number of viral genomes per cell under each condition. iLC and mLC populations derived from the progenitor cells of four different donors were exposed to BAC4 at an MOI of 10 PFU/cell for 15 min, 1 h, or 4 h. At each time point, cells were collected, washed, and stored (untreated) or washed and treated with citrate buffer for 1 min at room temperature or with proteinase K for 1 h at 4°C. After additional washes, cells were pelleted and subjected to real-time quantitative PCR with primers hybridizing to the viral UL122/123 ORF (79) or to the cellular albumin gene (63) and the number of viral genomes/cell was calculated.

At each of the time points tested, iLC contained slightly but consistently larger amounts of viral DNA than mLC did (Fig. 3A, white bars), with iLC/mLC ratios ranging from 2 ± 1.5 at 15 min postinfection to 3.8 ± 1 at 4 h postinfection (Fig. 3B, white bars). These values are higher than those obtained by IFA (Fig. 2J), likely because of the superior precision of the quantification method used (real-time PCR instead of manual counting), the testing of cell populations derived from four different CD34$^+$ cell donors instead of one, and the tracking of viral genomes instead of viral

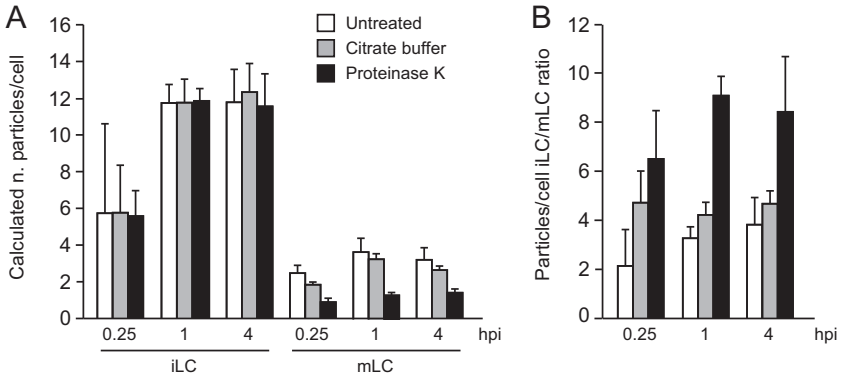

FIG 3 Viral genome contents of iLC and mLC at early times postinfection. iLC and mLC populations differentiated from the progenitor cells of four different CD34$^+$ cell donors were exposed to BAC4 at an MOI of 10 PFU/cell. At 0.25, 1, and 4 hpi, cells were collected, washed, and stored (untreated); washed and exposed to citrate buffer to inactivate nonpenetrating viral particles; or washed and treated with proteinase K to remove extracellular virions. Real-time quantitative PCR was then used to determine the number (n.) of viral genome copies per cell at each time postinfection (A) and to derive the ratio of the calculated number of viral genome copies present in iLC to the number present in mLC (B).

capsids. Treatment of infected cells with citrate buffer did not change the viral genome content of iLC and had only modest effects (25, 10, and 17% decrease from untreated samples at 0.25, 1, and 4 h, respectively) on mLC (Fig. 3A, gray bars), suggesting that, contrary to what was reported for other cell types (57, 76–78), exposure to a low pH did not completely remove nonpenetrating virions from infected LC. Identical results were obtained after iLC treatment with proteinase K, while enzymatic digestion of mLC resulted in the removal of 55 to 64% of the bound virions (Fig. 3A, black bars), consistent with what was previously reported for monocytes, fibroblasts, and epithelial cells (58, 59). Viral particle attachment and internalization may thus occur more efficiently in iLC than in mLC. Already at 15 min postinfection, virtually all of the virions bound to iLC are protected from proteolysis, presumably on account of their localization within the cell's interior. In contrast, only about 36 to 44% of the attached particles are internalized by mLC at each of the time points tested, suggesting that entry into mLC may be slower or less effective than entry into iLC. Because of these differences, the intracellular content of viral particles was consistently higher (6.5-fold ± 2-fold to 9-fold ± 0.7-fold) in iLC than in mLC at each time postinfection (Fig. 3B, black bars).

Together, these data indicate that virion entry into iLC occurs with similar or better efficiencies than virion entry into mLC, suggesting that defects in binding and penetration are not the main source of iLC resistance to infection.

Viral genome losses are similar in iLC and mLC. To determine if any difference might exist in the way viral particles are processes by each LC type after penetration, the fate of viral genomes over time was tracked in HFF and ARPE-19 cells, used as reference, and in iLC and mLC infected with BAC4, UL128mut, BADr, and AD169 at an MOI of 10 PFU/cell. Cells were exposed to each strain for 4 h before being washed with medium, treated with citrate buffer to inactivate residual nonpenetrating virus, and washed extensively again. Real-time quantitative PCR was then used to determine the number of viral genomes present in each cell population at 4, 8, 24, and 48 hpi and to calculate the proportion of genomes remaining at each time point relative to that at 4 hpi (Fig. 4), when the entry of noninternalized virions was halted by low-pH treatment. The calculated average number of viral genomes per cell found in each population at 4 hpi averaged 2.6 ± 1.8 in iLC, 1.3 ± 1.1 in mLC, 2.7 ± 2 in ARPE-19 cells, and 3.1 ± 3 in HFF. Again, at this early time postinfection, iLC appeared to hold more viral genomes than mLC did, while the viral DNA contents of HFF and ARPE-19 cells were almost identical.

As expected, all of the strains could efficiently infect HFF. The content of viral DNA remained largely the same in these cells from 4 to 24 hpi, until the onset of viral replication caused it to increase at 48 hpi (Fig. 4A, C, E, and G, dark gray bars). The same profile was observed in ARPE-19 cells infected with BAC4 and BADr (Fig. 4A and E, light gray bars), while genomes from UL128mut and AD169 were gradually lost over time with no amplification at 48 hpi (Fig. 4C and G, light gray bars). The detection of UL128mut and AD169 genomes in ARPE-19 cell samples at the early time of 8 hpi clearly indicates that at least virion binding, if not also penetration, can occur in these cells in the absence of the gH/gL/UL128-131A pentamer. The sharp drop in viral DNA amounts observed later on, however, reveals that the entry route used by these virions may not be viable, failing to lead to successful genome replication.

A gradual decline in the cellular content of viral genomes was observed in both LC types, irrespective of the strain used for infection (Fig. 4B, D, F, and H). This decrease was slightly more pronounced in mLC than in iLC, which retained approximately 50% more input (4 hpi) viral DNA than mLC did at 48 hpi, on average (Fig. 4J). As expected, because of the delayed CMV replication kinetics in mLC compared to those in HFF and ARPE-19 cells (30), no boost in viral DNA copy numbers was detected in mLC at 48 hpi. The fact that expression of the IE1/IE2 proteins could be detected at this same time point, however, indicates that the viral replication cycle had successfully started in these cells.

In summary, no substantial difference was detected in the cellular content of viral genomes after infection of LC with strains carrying functional or dysfunctional UL128-131A complexes, as shown by the relatively small standard deviations in Fig. 4J compared to those of ARPE-19 cells in Fig. 4I. This suggests that LC may process incoming virions from different strains in similar ways, leading to comparable proportions of infected cells (Fig. 1) and supporting the notion that the UL128, UL130, and UL131A proteins are not essential for LC infection. The extent of viral genome loss was larger in both LC types than in HFF or ARPE-19 cells (when exposed to BAC4 or BADr), but while enhanced genome loss may contribute to ARPE-19 cells' resistance to infection by certain strains (Fig. 4C and G), no obvious correlation could be found between the extent of genome retention in LC and the proportion of IE1/IE2$^+$ cells. Despite still containing 41% ± 10% of the input viral DNA at 48 hpi (Fig. 4J), only 3% ± 2% of the iLC (average of four donors) were IE1/IE2$^+$ (Fig. 4J); in contrast, mLC retained merely 20% ± 11% of the initial viral genomes, and yet, 14% ± 11% of them expressed the IE1/IE2 proteins. These data suggest that increased genome loss due to the degradation of viral DNA, the ejection of penetrated particles, or other unknown mechanisms may contribute to the decreased permissiveness of mLC compared to that of HFF or ARPE-19 cells but are not likely to be the prime source of iLC resistance.

Nuclear deposition of CMV genomes is occurring in iLC. We subsequently sought to establish if viral genomes did successfully reach the nuclei of iLC or if, instead, they remained trapped in the cell cytoplasm. High-magnification images of iLC harvested at 4 hpi with BAC4 and stained for pp150 showed the presence of numerous virions in close proximity to the nucleus (Fig. 5A). Confocal microscopy imaging further revealed the existence of what appeared to be points of contact between some viral particles and the outer surface of the nuclei of both iLC and mLC (Fig. 5B to E, arrows), suggesting that capsids could successfully dock to the nuclear envelope in both cell types. To determine if viral genomes were subsequently deposited into the nucleus, cytospin preparations of LC infected with BAC4 and harvested at 24 hpi were subjected to FISH labeling with probes hybridizing to the viral genome. Bright dots corresponding to viral DNA could be detected within the nuclei of both iLC and mLC (Fig. 5D to G), with no apparent difference between the two cell types with respect to genome localization or the number of genomes per nucleus. In fact, iLC and mLC samples could not be distinguished in blinded analyses of FISH slides, suggesting that nuclear deposition of viral genomes was occurring with similar efficiencies in both LC types.

The abundance of UL122/UL123 and UL50 transcripts is significantly lower in iLC. Finally, we sought to determine if transcription of the UL122/123 and UL50 ORFs was similarly efficient in iLC and mLC. The UL122/123 ORF is expressed with immedi-

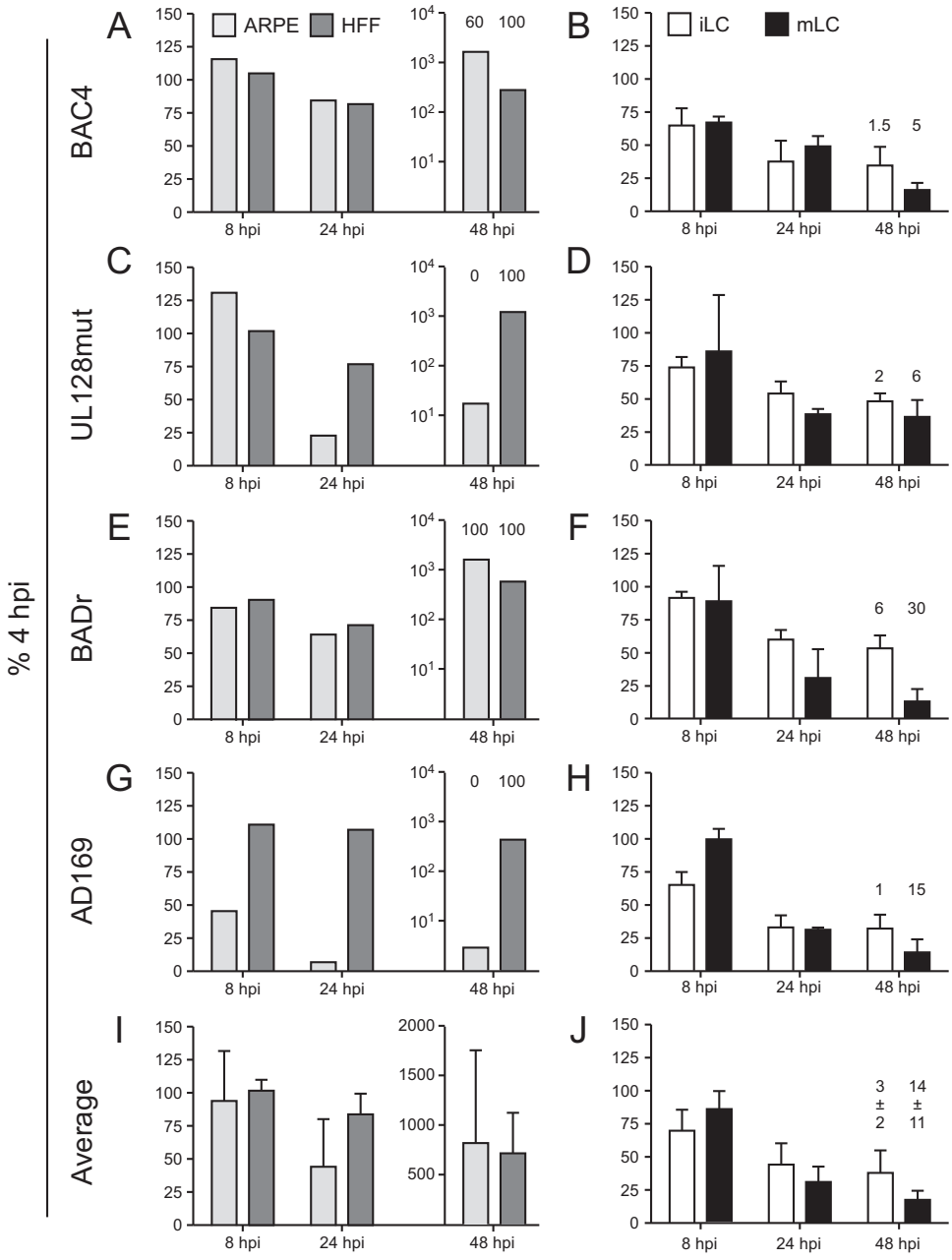

FIG 4 Viral genome contents of HFF, ARPE-19 cells, iLC, and mLC at later times postinfection. Cells were exposed to BAC4, UL128mut, BADr, or AD169 virions at an MOI of 10 PFU/cell for 4 h, washed in medium to remove the inoculum, and treated with citrate buffer to prevent any further virion penetration. A quarter of the cells were then harvested immediately (4 hpi), while the rest were plated and harvested at 8, 24, and 48 hpi. Real-time quantitative PCR was used to determine the number of viral genome copies per cell at each time point and to calculate the percentage of genomes remaining at 8, 24, and 48 hpi relative to that at 4 hpi (% 4 hpi). (A, C, E, and G) Genomes remaining in ARPE-19 cells and HFF from one representative experiment, with the 48-hpi values shown on a $\log_{10}$ scale. (B, D, F, and H) Mean percentages of genomes remaining in iLC and mLC derived from four different $CD34^+$ cell donors with standard deviations. (I and J) Mean percentages of genomes remaining in each population after infection with BAC4, UL128mut, BADr, and AD169 with standard deviations. Values above the columns at 48 hpi are the percentages of $IE1/IE2^+$ cells obtained in IFA analyses of each cell type at 48 hpi.

ate early kinetics and encodes the IE1 and IE2 proteins essential for infection onset (80–82), while the UL50 ORF is expressed with early kinetics and encodes the nuclear egress complex component UL50 (83–85). Real-time, quantitative reverse transcription-PCR was used to determine the numbers of UL122/123 and UL50 transcript copies present in each cell type at 24, 48, and 72 h postexposure to AD169, BADr, BAC4, or UL128mut and to calculate the ratio of the number of cDNA copies of each gene present in the mLC to the number of copies in the iLC of each donor (Fig. 6).

Although the UL122/123 ORF was expressed in both cell types, mLC consistently contained more transcript copies than iLC at each time point. Already at 24 hpi, the number of UL122/123 mRNA copies in mLC was 6 times (AD169 and BAC4), 8 times (UL128mut), and 12 times (BADr) greater than that in iLC

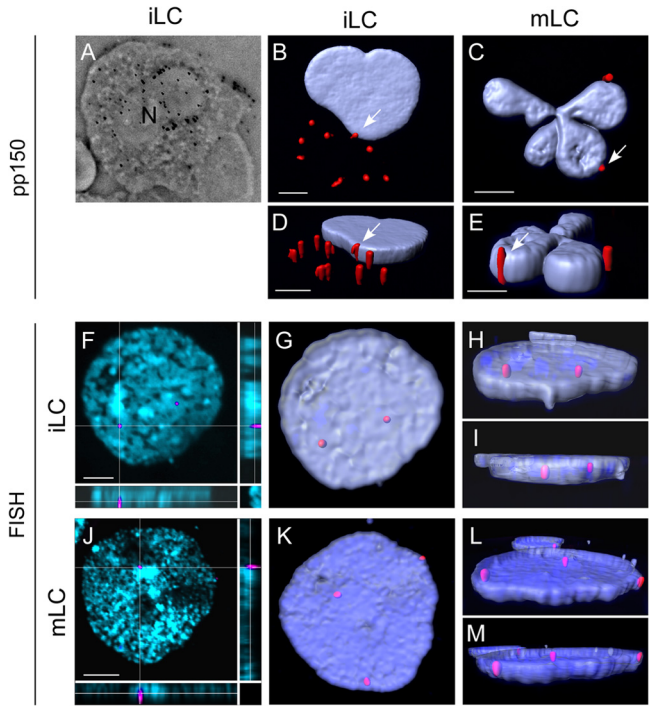

FIG 5 Localization of viral particles and genomes within iLC and mLC. Cells were exposed to BAC4 at an MOI of 10 PFU/cell, harvested at 4 hpi (A to E) or 24 hpi (F to M), and processed by IFA with anti-pp150 antibodies (A to E) or by FISH with probes hybridizing to the viral genome (F to M). (A) Superimposition of light and fluorescence images of an infected iLC. The signal from pp150$^+$ viral particles appears as sharp black dots. N, nucleus. Original magnification, ×60. (B to E) Confocal microscopy images of infected iLC and mLC stained with anti-pp150 antibodies (red signal) and with Hoechst 33345 (light blue signal). Merged z-stack images were processed with the Imaris Surpass Surfaces visualization tool to create an artificial solid-object representation of specified gray value ranges in the data set. Images are shown frontwise in panels B and C and rotated leftwise and tilted at an ~45° angle in panels D and E. The total z-stack thickness of the iLC sample was 2.45 μm, while the mLC sample measured 3.51 μm. Arrows point at viral particles that appear to be in close contact with the nuclear envelope. Original magnification, ×63. Bars, 5 μm. (F to M) Confocal microscopy images of infected iLC and mLC stained with a ChromaTide Alexa Fluor 594-labeled probe hybridizing to multiple different regions of the viral genome (red signal) and with Hoechst 33345 (light blue signal). The merged images in panels F and J were processed with the Surpass Section visualization tool to display the frontal (x, y, main square) and orthogonal (x, z, bottom rectangle) and (y, z, right rectangle) views of the z stack, while the images in panels G to I and K to M were processed with the Surpass Surfaces visualization tool and show nuclei frontwise in panels G and K, tilted at an ~30° angle in panels H and L, and tilted at an ~90° angle in panels I and M. The total z-stack thickness of both samples was 1.43 μm. Original magnification, ×63.

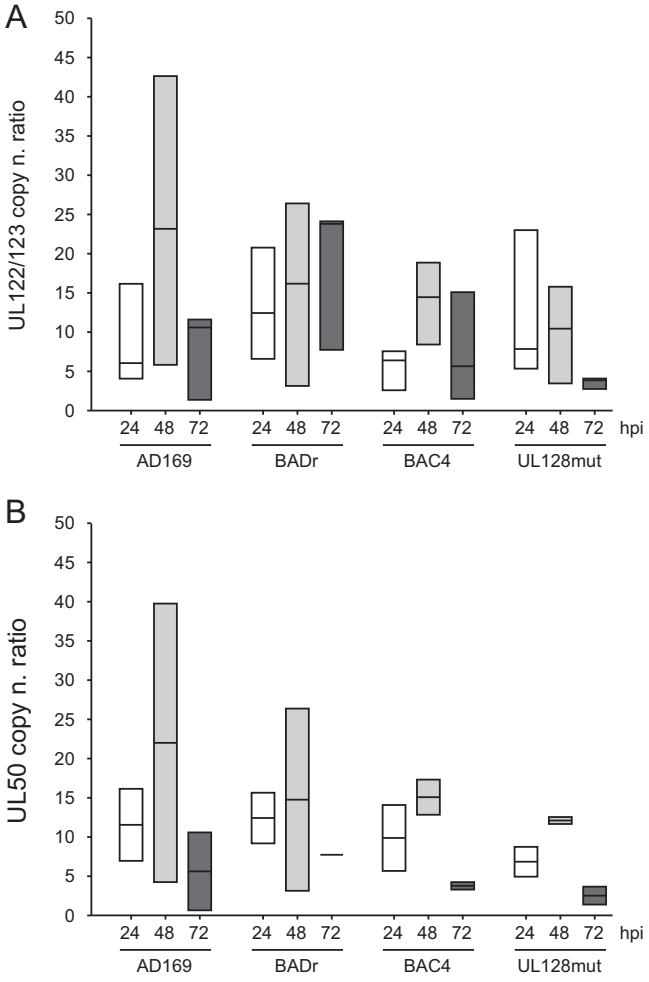

FIG 6 Ratios of UL122/123 and UL50 transcript amounts present in infected iLC and mLC. mRNA extracted from cells exposed to AD169, BADr, BAC4, or UL128mut at an MOI of 10 PFU/cell and harvested at 24, 48, and 72 hpi was DNase treated and reverse transcribed. Quantitative real-time PCR assays were then used to quantify the number (n.) of UL122/123 and UL50 cDNA copies present in the equivalent of 1×10^2 iLC or mLC per reaction and to calculate the ratio of the copy amounts found in mLC to those detected in iLC differentiated from the progenitor cells of three or four (UL122/123, A) and two (UL50, B) different CD34$^+$ progenitor cell donors. Each floating vertical bar extends from the minimum to the maximum ratio obtained for the iLC and mLC from different donors at each time point, while a horizontal bar marks the median value of each group.

(Fig. 6A, white bars). These differences further increased for two donors at 48 hpi (43- and 40-fold in AD169-infected cells, 26- and 25-fold in BADr-infected cells) while remaining close to 5-fold for the other two. An increase was also detected after infection with BAC4 (14-fold) and UL128mut (10-fold) (Fig. 6A, light gray bars). Finally, the ratios remained high at 72 hpi, with median values of 10-fold (AD169) and 24-fold (BADr), while decreasing back to 6-fold and 4-fold after infection with BAC4 and UL128mut, respectively (Fig. 6A, dark gray bars).

Similar results were obtained for UL50 in LC populations derived from the CD34$^+$ cells of two donors. Consistent with data from infected fibroblasts (83), UL50 was expressed at 24 hpi in both LC types, albeit at different levels (median mLC/iLC ratios of 11 in AD169, 12 in BADr, 10 in BAC4, and 7 in UL128mut infections, Fig. 6B, white bars). While the number of UL50 mRNA copies in mLC remained at least 5-fold higher than that in iLC at each time point after infection with AD169 or BADr, differences were somewhat lower at 72 h after infection with BAC4 and UL128mut (Fig. 6B, dark gray bars). Considering that at both 24 and 48 h after infection with each strain, iLC contain more viral genomes than mLC (Fig. 4B, D, F, and H) but substantially less UL122/123 and UL50 mRNA copies (Fig. 6), transcription of viral genes in iLC appears to be highly restricted. Together, these data identify viral gene transcription as the first severely impaired step in the regular progression of the viral cycle in iLC.

DISCUSSION

Efficient CMV penetration of specific cell types requires fusion of the virion envelope with cellular membranes in a process controlled by both viral and cellular factors. Capsid release into the cytoplasm can indeed occur at the periphery of the cell or from intracellular vesicles, depending on the complement of glycoprotein complexes displayed on the virion surface and on the cell type.

The gH/gL/UL128-131A complex was shown to promote entry by endocytosis and to be essential for the infection of epithelial cells, endothelial cells, monocytes, and iMDDC (38, 40, 45, 59, 67, 86). Exposure to strains carrying only the gH/gL/gO complex was not followed by viral gene expression in these cells, implying that endocytosis is likely the predominant, if not the only, entry pathway conducive to productive infection onset.

Consistent with this, we found that viral DNA maintenance and replication, as well as IE1/IE2 protein expression, in ARPE-19 epithelial cells occurred only after infection with strains possessing the pentameric complex and presumably entering by endocytosis (Table 2 and Fig. 4).

In contrast to the infection of epithelial cells, that of HFF does not require expression of the UL128, UL130, and UL131A proteins but depends on the presence of the gH/gL/gO complex to support fusion of the viral envelope with the plasma membrane (46, 72, 87, 88). In our assays, penetration of HFF by virions from strains possessing or lacking the gH/gL/UL128-131A complex progressed equally well and led to the onset of productive infections (Fig. 4A, C, E, and G), suggesting that both entry modes may be allowed to occur in this cell type. Alternatively, virions of strains harboring both complexes on their envelope, such as BAC4 and BADr, may selectively use the trimeric complex to access HFF. While the intracellular release of naked capsids at the cell periphery is considered to be the main entry route of CMV into these cells (88), incoming virions were also detected within phagolysosome-like vacuoles in electron microscopic images of infected cells (89), suggesting that endocytosis of viral particles can also take place in HFF.

Here we show that the pentameric complex is not required for infection of iLC and mLC, although in its presence, the efficiency of mLC infection was increased by about 2-fold (Fig. 1). Similar to the situation in HFF, strains containing both complexes or just gH/gL/gO were equally able to bind to and likely enter both types of LC, but their genomic DNA was subsequently lost (Fig. 4B, D, F, and H), in a fashion comparable to that of UL128mut and AD169 in ARPE-19 cells (Fig. 4C and G). In contrast to the latter, however, the rate and extent of viral genome loss were similar for all strains (Fig. 4J) and were not accompanied by a complete absence of IE1/IE2 gene expression in mLC (Fig. 4J and 1B). It is thus possible that, akin to HFF, both endocytosis and fusion with the plasma membrane are viable routes of entry into iLC and mLC and may be used interchangeably by virions possessing both complexes. When only the gH/gL/gO complex is present, particles may still use both pathways to access cells, as suggested by the lack of difference between the intracellular contents of viral DNA of different strains. Because the endocytic pathway is impracticable in the absence of the pentameric complex, a portion of these virions may fail to reach the nucleus, leading to a reduction in the percentage of IE1/IE2$^+$ mLC.

Our finding that mLC are consistently more permissive to infection than iLC are (Fig. 1) (30) is in stark contrast to the situation with MDDC, whereby immature cells, and not their mature counterparts, are the most susceptible to CMV infection (33–36). Despite being related and sharing many of the features and functions typical of antigen-presenting cells, LC and MDDC respond to CMV in opposite ways, reflecting the heterogeneity and functional specialization of different DC populations. If these differences observed *in vitro* are also mirrored *in vivo*, then dermal DC and epidermal LC are likely to play dramatically different roles in the development of CMV pathogenesis and in the generation of antiviral immune responses, a concept that may be relevant for the development of live-attenuated vaccines intended for delivery via mucosal surfaces.

None of the CMV strains tested so far has the ability to initiate productive infections in iLC. This strongly supports the existence of some iLC-specific defense mechanism that cannot be overcome by any viral countermeasure. Intriguingly, while entry is the target of multiple cellular antiviral strategies restricting infection in different cell types, CMV penetration of iLC is not blocked. Quite to the contrary, data from our particle neutralization/detachment experiments indicate that virion internalization is more efficient in iLC than in mLC (Fig. 3A), leading to higher, instead of lower, intracellular contents of virions at early times postinfection (Fig. 3B).

This finding may not be that surprising in view of the well-known superior antigen-capturing abilities of iLC, compared to mLC (25, 90). While all three antigen internalization pathways, namely, macropinocytosis, endocytosis, and phagocytosis, are fully operational in iLC, two (macropinocytosis and phagocytosis) are downregulated during maturation (91, 92), leaving endocytosis as the predominant means of extracellular material acquisition by mLC. While our data suggest that CMV entry into mLC may occur independently of vesicle-mediated transport pathways (Fig. 1), the loss of two prominent entry routes following maturation may negatively impact the efficiency of CMV penetration of these cells, at least in the case of pentamer-containing strains such as BAC4.

Subsequent to entry, no major differences were detected between iLC and mLC in the kinetics of viral genome loss (Fig. 4J) or in the number of viral genomes reaching the nucleus, arguing against enhanced virion degradation or inefficient nuclear deposition of viral genomes as the main cause of iLC resistance to infection. In contrast, the abundance of UL122/123 and UL50 ORFs transcripts was considerably lower in iLC than in mLC at each of the times tested (Fig. 6), pointing at viral gene transcription as the first severely restricted step in the regular progression of the viral cycle.

The most intriguing question now is how viral gene transcription is blocked in iLC. It is, of course, possible for iLC to express higher levels of specific transcriptional repressors, whose binding to the major immediate early promoter (MIEP) is followed by the severe inhibition of UL122/123 expression. Conversely, mLC may contain higher levels of transcriptional activators, whose positive activity on the MIEP may promote the onset of lytic infection. The resistance to CMV infection of undifferentiated human monocytic THP-1 cells, for instance, was found to be partially due to the presence of the MBF1 and MRF transcriptional repressors in large amounts (93, 94). Upon THP-1 differentiation into macrophages, the abundance of both factors was substantially reduced, with a concomitant increase in MIEP activity. This allowed the expres-

sion of the IE1/IE2 proteins and initiation of the viral replication cycle to occur (93, 94). Epigenetically acting proteins such as histone acetyltransferases, histone deacetylases, and histone methyltransferases may also be potential players. In latently infected $CD34^+$ progenitor cells, the transcriptionally inactive UL122/123 promoter was indeed found to be associated with deacetylated H4 histones and with the transcriptional repressor heterochromatin protein 1 (HP1), while in mLC derived from latently infected progenitors and harboring reactivating virus, the now active UL122/123 promoter was associated with acetylated H4 histones and had lost HP1 binding (15–17). Interestingly, and similar to our findings with directly infected iLC, no expression of the viral UL122/123 ORFs was detected in iLC differentiated from latently infected $CD34^+$ cells, indicating that maturation is crucial for both infection onset and viral reactivation to occur. Thus, although CMV reactivation in the $CD34^+$-LC model was proposed to be "differentiation dependent" (95), we believe that it may be more tightly linked to the process of maturation (i.e., "maturation dependent"). Interestingly, while differentiation and maturation of latently infected $CD34^+$ progenitors into mLC trigger viral reactivation (15, 16), maturation of directly infected iLC has not yet been reported to yield infectious virus. This suggests that the mechanisms mediating silencing of the MIEP in iLC derived from latently infected progenitors may be different from those acting after direct infection of these cells.

Finally, mLC susceptibility to direct infection, as well as the establishment of viral latency in $CD34^+$ cells, was also proposed to be regulated by the activity of nuclear domain 10 (ND10) bodies (96), whose negative effects on MIEP transcription (97–99) can be partially reversed by the nuclear delivery of the viral tegument protein pp71 (100–105). Although no evidence was provided by Saffert et al. as to the actual presence of viral genomes within the ND10 bodies of infected $CD34^+$ cells or mLC (96), pp71 appeared to reach the nucleus in at least a few infected mLC. If incoming viral genomes are indeed sequestered within the ND10 bodies of iLC and if pp71 is subsequently prevented from reaching the nucleus, then silencing of the MIEP may remain in effect, preventing the expression of the UL122/123 ORFs in these cells. On the other hand, depletion of the ND10 component and the strong transcriptional repressor hDaxx from nonpermissive human teratocarcinoma T2 cells did not render them susceptible to infection (106), and neither was their loss of resistance (triggered by exposure to vasoactive intestinal peptide) accompanied by hDaxx degradation (107), suggesting that the role played by hDaxx and pp71 in controlling CMV infection onset may be cell dependent and that they may not be active in iLC.

Altogether, we postulate that iLC resistance to infection is highly unlikely to depend on the activity of single cellular proteins. Instead, multiple host defense effectors may cooperate in generating an unfavorable environment for viral gene transcription. Conversely, mLC susceptibility to CMV infection and reactivation may depend on the assembly of an intranuclear milieu conducive to MIEP activation and be characterized by the presence of selected transcription factors, the absence of others, and the occurrence of specific epigenetic modifications of the viral and cellular genomes (95, 108). The relative contributions of some of these elements to the regulation of LC susceptibility to infection are under investigation.

ACKNOWLEDGMENTS

We thank Michael McVoy, C. Sinzger, and E. S. Mocarski for their generous gifts of virus strains and cell lines. We also thank Keith Quirolo, Clinical Director of the Apheresis Program at the Children's Hospital & Research Center Oakland, for providing us with part of the peripheral blood samples used in this work to isolate hematopoietic progenitor cells.

This work was supported by NIH grants AI088481 and AI099372 to L.H. and by a subgrant to L.H. from the Canadian Institutes of Health Research.

REFERENCES

1. **Banchereau J, Steinman RM.** 1998. Dendritic cells and the control of immunity. Nature **392:**245–252. http://dx.doi.org/10.1038/32588.
2. **Lee HK, Iwasaki A.** 2007. Innate control of adaptive immunity: dendritic cells and beyond. Semin. Immunol. **19:**48–55. http://dx.doi.org/10.1016/j.smim.2006.12.001.
3. **Teunissen MB, Haniffa M, Collin MP.** 2012. Insight into the immunobiology of human skin and functional specialization of skin dendritic cell subsets to innovate intradermal vaccination design. Curr. Top. Microbiol. Immunol. **351:**25–76. http://dx.doi.org/10.1007/82_2011_169.
4. **Iwasaki A.** 2007. Mucosal dendritic cells. Annu. Rev. Immunol. **25:**381–418. http://dx.doi.org/10.1146/annurev.immunol.25.022106.141634.
5. **Steinman RM.** 2007. Dendritic cells: understanding immunogenicity. Eur. J. Immunol. **37**(Suppl. 1)**:**S53–S60. http://dx.doi.org/10.1002/eji.200737400.
6. **Kis Z, Pallinger E, Endresz V, Burian K, Jelinek I, Gonczol E, Valyi-Nagy I.** 2004. The interactions between human dendritic cells and microbes; possible clinical applications of dendritic cells. Inflamm. Res. **53:**413–423. http://dx.doi.org/10.1007/s00011-004-1274-0.
7. **Mocarski ES, Shenk T, Pass RF.** 2007. Cytomegaloviruses, p 2701–2772. *In* Knipe DM, Howley PM (ed), Fields virology. Lippincott Williams & Wilkins, Philadelphia, PA.
8. **Britt W.** 2008. Manifestations of human cytomegalovirus infection: proposed mechanisms of acute and chronic disease. Curr. Top. Microbiol. Immunol. **325:**417–470. http://dx.doi.org/10.1007/978-3-540-77349-8_23.
9. **Crough T, Khanna R.** 2009. Immunobiology of human cytomegalovirus: from bench to bedside. Clin. Microbiol. Rev. **22:**76–98. http://dx.doi.org/10.1128/CMR.00034-08.
10. **Sinclair J.** 2008. Manipulation of dendritic cell functions by human cytomegalovirus. Expert Rev. Mol. Med. **10:**e35. http://dx.doi.org/10.1017/S1462399408000872.
11. **Rölle A, Olweus J.** 2009. Dendritic cells in cytomegalovirus infection: viral evasion and host countermeasures. APMIS **117:**413–426. http://dx.doi.org/10.1111/j.1600-0463.2009.02449.x.
12. **Minton EJ, Tysoe C, Sinclair JH, Sissons JG.** 1994. Human cytomegalovirus infection of the monocyte/macrophage lineage in bone marrow. J. Virol. **68:**4017–4021.
13. **Hahn G, Jores R, Mocarski ES.** 1998. Cytomegalovirus remains latent in a common precursor of dendritic and myeloid cells. Proc. Natl. Acad. Sci. U. S. A. **95:**3937–3942. http://dx.doi.org/10.1073/pnas.95.7.3937.
14. **Sinclair J.** 2008. Human cytomegalovirus: latency and reactivation in the myeloid lineage. J. Clin. Virol. **41:**180–185. http://dx.doi.org/10.1016/j.jcv.2007.11.014.
15. **Reeves MB, Lehner PJ, Sissons JG, Sinclair JH.** 2005. An in vitro model for the regulation of human cytomegalovirus latency and reactivation in dendritic cells by chromatin remodelling. J. Gen. Virol. **86:**2949–2954. http://dx.doi.org/10.1099/vir.0.81161-0.
16. **Reeves MB, MacAry PA, Lehner PJ, Sissons JG, Sinclair JH.** 2005. Latency, chromatin remodeling, and reactivation of human cytomegalovirus in the dendritic cells of healthy carriers. Proc. Natl. Acad. Sci. U. S. A. **102:**4140–4145. http://dx.doi.org/10.1073/pnas.0408994102.
17. **Reeves MB, Sinclair JH.** 2010. Analysis of latent viral gene expression in natural and experimental latency models of human cytomegalovirus and its correlation with histone modifications at a latent promoter. J. Gen. Virol. **91:**599–604. http://dx.doi.org/10.1099/vir.0.015602-0.
18. **Huang MM, Kew VG, Jestice K, Wills MR, Reeves MB.** 2012. Efficient human cytomegalovirus reactivation is maturation dependent in the Langerhans dendritic cell lineage and can be studied using a $CD14^+$ experimental latency model. J. Virol. **86:**8507–8515. http://dx.doi.org/10.1128/JVI.00598-12.
19. **Feng P, Yee KK, Rawson NE, Feldman LM, Feldman RS, Breslin PA.**

2009. Immune cells of the human peripheral taste system: dominant dendritic cells and CD4 T cells. Brain Behav. Immun. **23:**760–766. http://dx.doi.org/10.1016/j.bbi.2009.02.016.
20. **Jahnsen FL, Gran E, Haye R, Brandtzaeg P.** 2004. Human nasal mucosa contains antigen-presenting cells of strikingly different functional phenotypes. Am. J. Respir. Cell Mol. Biol. **30:**31–37. http://dx.doi.org/10.1165/rcmb.2002-0230OC.
21. **Allam JP, Niederhagen B, Bucheler M, Appel T, Betten H, Bieber T, Berge S, Novak N.** 2006. Comparative analysis of nasal and oral mucosa dendritic cells. Allergy **61:**166–172. http://dx.doi.org/10.1111/j.1398-9995.2005.00965.x.
22. **Allam JP, Stojanovski G, Friedrichs N, Peng W, Bieber T, Wenzel J, Novak N.** 2008. Distribution of Langerhans cells and mast cells within the human oral mucosa: new application sites of allergens in sublingual immunotherapy? Allergy **63:**720–727. http://dx.doi.org/10.1111/j.1398-9995.2007.01611.x.
23. **Strobl H, Bello-Fernandez C, Riedl E, Pickl WF, Majdic O, Lyman SD, Knapp W.** 1997. flt3 ligand in cooperation with transforming growth factor-beta1 potentiates in vitro development of Langerhans-type dendritic cells and allows single-cell dendritic cell cluster formation under serum-free conditions. Blood **90:**1425–1434.
24. **Strobl H, Riedl E, Scheinecker C, Bello-Fernandez C, Pickl WF, Rappersberger K, Majdic O, Knapp W.** 1996. TGF-beta 1 promotes in vitro development of dendritic cells from $CD34^+$ hemopoietic progenitors. J. Immunol. **157:**1499–1507.
25. **Banchereau J, Briere F, Caux C, Davoust J, Lebecque S, Liu YJ, Pulendran B, Palucka K.** 2000. Immunobiology of dendritic cells. Annu. Rev. Immunol. **18:**767–811. http://dx.doi.org/10.1146/annurev.immunol.18.1.767.
26. **Liu YJ.** 2001. Dendritic cell subsets and lineages, and their functions in innate and adaptive immunity. Cell **106:**259–262. http://dx.doi.org/10.1016/S0092-8674(01)00456-1.
27. **van der Aar AM, Sylva-Steenland RM, Bos JD, Kapsenberg ML, de Jong EC, Teunissen MB.** 2007. Loss of TLR2, TLR4, and TLR5 on Langerhans cells abolishes bacterial recognition. J. Immunol. **178:**1986–1990. http://www.jimmunol.org/content/178/4/1986.long.
28. **Osugi Y, Vuckovic S, Hart DN.** 2002. Myeloid blood CD11c(+) dendritic cells and monocyte-derived dendritic cells differ in their ability to stimulate T lymphocytes. Blood **100:**2858–2866. http://dx.doi.org/10.1182/blood.V100.8.2858.
29. **Burster T, Beck A, Tolosa E, Schnorrer P, Weissert R, Reich M, Kraus M, Kalbacher H, Haring HU, Weber E, Overkleeft H, Driessen C.** 2005. Differential processing of autoantigens in lysosomes from human monocyte-derived and peripheral blood dendritic cells. J. Immunol. **175:**5940–5949. http://www.jimmunol.org/content/175/9/5940.long.
30. **Hertel L, Lacaille VG, Strobl H, Mellins ED, Mocarski ES.** 2003. Susceptibility of immature and mature Langerhans cell-type dendritic cells to infection and immunomodulation by human cytomegalovirus. J. Virol. **77:**7563–7574. http://dx.doi.org/10.1128/JVI.77.13.7563-7574.2003.
31. **Riegler S, Hebart H, Einsele H, Brossart P, Jahn G, Sinzger C.** 2000. Monocyte-derived dendritic cells are permissive to the complete replicative cycle of human cytomegalovirus. J. Gen. Virol. **81:**393–399. http://vir.sgmjournals.org/content/81/2/393.long.
32. **Raftery MJ, Schwab M, Eibert SM, Samstag Y, Walczak H, Schonrich G.** 2001. Targeting the function of mature dendritic cells by human cytomegalovirus: a multilayered viral defense strategy. Immunity **15:**997–1009. http://dx.doi.org/10.1016/S1074-7613(01)00239-4.
33. **Moutaftsi M, Mehl AM, Borysiewicz LK, Tabi Z.** 2002. Human cytomegalovirus inhibits maturation and impairs function of monocyte-derived dendritic cells. Blood **99:**2913–2921. http://dx.doi.org/10.1182/blood.V99.8.2913.
34. **Grigoleit U, Riegler S, Einsele H, Laib Sampaio K, Jahn G, Hebart H, Brossart P, Frank F, Sinzger C.** 2002. Human cytomegalovirus induces a direct inhibitory effect on antigen presentation by monocyte-derived immature dendritic cells. Br. J. Haematol. **119:**189–198. http://dx.doi.org/10.1046/j.1365-2141.2002.03798.x.
35. **Beck K, Meyer-Konig U, Weidmann M, Nern C, Hufert FT.** 2003. Human cytomegalovirus impairs dendritic cell function: a novel mechanism of human cytomegalovirus immune escape. Eur. J. Immunol. **33:**1528–1538. http://dx.doi.org/10.1002/eji.200323612.
36. **Sénéchal B, Boruchov AM, Reagan JL, Hart DN, Young JW.** 2004. Infection of mature monocyte-derived dendritic cells with human cytomegalovirus inhibits stimulation of T-cell proliferation via the release of soluble CD83. Blood **103:**4207–4215. http://dx.doi.org/10.1182/blood-2003-12-4350.
37. **Hahn G, Revello MG, Patrone M, Percivalle E, Campanini G, Sarasini A, Wagner M, Gallina A, Milanesi G, Koszinowski U, Baldanti F, Gerna G.** 2004. Human cytomegalovirus UL131-128 genes are indispensable for virus growth in endothelial cells and virus transfer to leukocytes. J. Virol. **78:**10023–10033. http://dx.doi.org/10.1128/JVI.78.18.10023-10033.2004.
38. **Wang D, Shenk T.** 2005. Human cytomegalovirus virion protein complex required for epithelial and endothelial cell tropism. Proc. Natl. Acad. Sci. U. S. A. **102:**18153–18158. http://dx.doi.org/10.1073/pnas.0509201102.
39. **Wang D, Shenk T.** 2005. Human cytomegalovirus UL131 open reading frame is required for epithelial cell tropism. J. Virol. **79:**10330–10338. http://dx.doi.org/10.1128/JVI.79.16.10330-10338.2005.
40. **Straschewski S, Patrone M, Walther P, Gallina A, Mertens T, Frascaroli G.** 2011. Protein pUL128 of human cytomegalovirus is necessary for monocyte infection and blocking of migration. J. Virol. **85:**5150–5158. http://dx.doi.org/10.1128/JVI.02100-10.
41. **Schuessler A, Sampaio KL, Straschewski S, Sinzger C.** 2012. Mutational mapping of pUL131A of human cytomegalovirus emphasizes its central role for endothelial cell tropism. J. Virol. **86:**504–512. http://dx.doi.org/10.1128/JVI.05354-11.
42. **Schuessler A, Sampaio KL, Scrivano L, Sinzger C.** 2010. Mutational mapping of UL130 of human cytomegalovirus defines peptide motifs within the C-terminal third as essential for endothelial cell infection. J. Virol. **84:**9019–9026. http://dx.doi.org/10.1128/JVI.00572-10.
43. **Schuessler A, Sampaio KL, Sinzger C.** 2008. Charge cluster-to-alanine scanning of UL128 for fine tuning of the endothelial cell tropism of human cytomegalovirus. J. Virol. **82:**11239–11246. http://dx.doi.org/10.1128/JVI.01069-08.
44. **Ryckman BJ, Rainish BL, Chase MC, Borton JA, Nelson JA, Jarvis MA, Johnson DC.** 2008. Characterization of the human cytomegalovirus gH/gL/UL128-131 complex that mediates entry into epithelial and endothelial cells. J. Virol. **82:**60–70. http://dx.doi.org/10.1128/JVI.01910-07.
45. **Gerna G, Percivalle E, Lilleri D, Lozza L, Fornara C, Hahn G, Baldanti F, Revello MG.** 2005. Dendritic-cell infection by human cytomegalovirus is restricted to strains carrying functional UL131-128 genes and mediates efficient viral antigen presentation to $CD8^+$ T cells. J. Gen. Virol. **86:**275–284. http://dx.doi.org/10.1099/vir.0.80474-0.
46. **Huber MT, Compton T.** 1998. The human cytomegalovirus UL74 gene encodes the third component of the glycoprotein H-glycoprotein L-containing envelope complex. J. Virol. **72:**8191–8197.
47. **Adler B, Scrivano L, Ruzcics Z, Rupp B, Sinzger C, Koszinowski U.** 2006. Role of human cytomegalovirus UL131A in cell type-specific virus entry and release. J. Gen. Virol. **87:**2451–2460. http://dx.doi.org/10.1099/vir.0.81921-0.
48. **Lee AW, Hertel L, Louie RK, Burster T, Lacaille V, Pashine A, Abate DA, Mocarski ES, Mellins ED.** 2006. Human cytomegalovirus alters localization of MHC class II and dendrite morphology in mature Langerhans cells. J. Immunol. **177:**3960–3971. http://www.jimmunol.org/content/177/6/3960.long.
49. **Lee AW, Wang N, Hornell TM, Harding JJ, Deshpande C, Hertel L, Lacaille V, Pashine A, Macaubas C, Mocarski ES, Mellins ED.** 2011. Human cytomegalovirus decreases constitutive transcription of MHC class II genes in mature Langerhans cells by reducing CIITA transcript levels. Mol. Immunol. **48:**1160–1167. http://dx.doi.org/10.1016/j.molimm.2011.02.010.
50. **Chee MS, Bankier AT, Beck S, Bohni R, Brown CM, Cerny R, Horsnell T, Hutchison CA, III, Kouzarides T, Martignetti JA, et al.** 1990. Analysis of the protein-coding content of the sequence of human cytomegalovirus strain AD169. Curr. Top. Microbiol. Immunol. **154:**125–169. http://dx.doi.org/10.1007/978-3-642-74980-3_6.
51. **Plotkin SA, Higgins R, Kurtz JB, Morris PJ, Campbell DA, Jr, Shope TC, Spector SA, Dankner WM.** 1994. Multicenter trial of Towne strain attenuated virus vaccine in seronegative renal transplant recipients. Transplantation **58:**1176–1178. http://dx.doi.org/10.1097/00007890-199412000-00006.
52. **Smith IL, Taskintuna I, Rahhal FM, Powell HC, Ai E, Mueller AJ, Spector SA, Freeman WR.** 1998. Clinical failure of CMV retinitis with intravitreal cidofovir is associated with antiviral resistance. Arch. Ophthalmol. **116:**178–185. http://dx.doi.org/10.1001/archopht.116.2.178.
53. **Murphy E, Yu D, Grimwood J, Schmutz J, Dickson M, Jarvis MA,**

Hahn G, Nelson JA, Myers RM, Shenk TE. 2003. Coding potential of laboratory and clinical strains of human cytomegalovirus. Proc. Natl. Acad. Sci. U. S. A. **100:**14976–14981. http://dx.doi.org/10.1073/pnas.2136652100.
54. **Yu D, Smith GA, Enquist LW, Shenk T.** 2002. Construction of a self-excisable bacterial artificial chromosome containing the human cytomegalovirus genome and mutagenesis of the diploid TRL/IRL13 gene. J. Virol. **76:**2316–2328. http://dx.doi.org/10.1128/jvi.76.5.2316-2328.2002.
55. **Wang D, Bresnahan W, Shenk T.** 2004. Human cytomegalovirus encodes a highly specific RANTES decoy receptor. Proc. Natl. Acad. Sci. U. S. A. **101:**16642–16647. http://dx.doi.org/10.1073/pnas.0407233101.
56. **Sinzger C, Hahn G, Digel M, Katona R, Sampaio KL, Messerle M, Hengel H, Koszinowski U, Brune W, Adler B.** 2008. Cloning and sequencing of a highly productive, endotheliotropic virus strain derived from human cytomegalovirus TB40/E. J. Gen. Virol. **89:**359–368. http://dx.doi.org/10.1099/vir.0.83286-0.
57. **Tirabassi RS, Enquist LW.** 1998. Role of envelope protein gE endocytosis in the pseudorabies virus life cycle. J. Virol. **72:**4571–4579.
58. **Chan G, Nogalski MT, Yurochko AD.** 2009. Activation of EGFR on monocytes is required for human cytomegalovirus entry and mediates cellular motility. Proc. Natl. Acad. Sci. U. S. A. **106:**22369–22374. http://dx.doi.org/10.1073/pnas.0908787106.
59. **Ryckman BJ, Jarvis MA, Drummond DD, Nelson JA, Johnson DC.** 2006. Human cytomegalovirus entry into epithelial and endothelial cells depends on genes UL128 to UL150 and occurs by endocytosis and low-pH fusion. J. Virol. **80:**710–722. http://dx.doi.org/10.1128/JVI.80.2.710-722.2006.
60. **Ogawa-Goto K, Tanaka K, Gibson W, Moriishi E, Miura Y, Kurata T, Irie S, Sata T.** 2003. Microtubule network facilitates nuclear targeting of human cytomegalovirus capsid. J. Virol. **77:**8541–8547. http://dx.doi.org/10.1128/JVI.77.15.8541-8547.2003.
61. **Spaete RR, Mocarski ES.** 1985. Regulation of cytomegalovirus gene expression: alpha and beta promoters are *trans* activated by viral functions in permissive human fibroblasts. J. Virol. **56:**135–143.
62. **Miller MS, Furlong WE, Pennell L, Geadah M, Hertel L.** 2010. RASCAL is a new human cytomegalovirus-encoded protein that localizes to the nuclear lamina and in cytoplasmic vesicles at late times postinfection. J. Virol. **84:**6483–6496. http://dx.doi.org/10.1128/JVI.02462-09.
63. **Bressollette-Bodin C, Coste-Burel M, Besse B, Andre-Garnier E, Ferre V, Imbert-Marcille BM.** 2009. Cellular normalization of viral DNA loads on whole blood improves the clinical management of cytomegalovirus or Epstein-Barr virus infections in the setting of pre-emptive therapy. J. Med. Virol. **81:**90–98. http://dx.doi.org/10.1002/jmv.21334.
64. **Ryckman BJ, Chase MC, Johnson DC.** 2010. Human cytomegalovirus TR strain glycoprotein O acts as a chaperone promoting gH/gL incorporation into virions but is not present in virions. J. Virol. **84:**2597–2609. http://dx.doi.org/10.1128/JVI.02256-09.
65. **Zhou M, Yu Q, Wechsler A, Ryckman BJ.** 2013. Comparative analysis of gO isoforms reveals that strains of human cytomegalovirus differ in the ratio of gH/gL/gO and gH/gL/UL128-131 in the virion envelope. J. Virol. **87:**9680–9690. http://dx.doi.org/10.1128/JVI.01167-13.
66. **Scrivano L, Sinzger C, Nitschko H, Koszinowski UH, Adler B.** 2011. HCMV spread and cell tropism are determined by distinct virus populations. PLoS Pathog. **7:**e1001256. http://dx.doi.org/10.1371/journal.ppat.1001256.
67. **Wang D, Yu QC, Schroer J, Murphy E, Shenk T.** 2007. Human cytomegalovirus uses two distinct pathways to enter retinal pigmented epithelial cells. Proc. Natl. Acad. Sci. U. S. A. **104:**20037–20042. http://dx.doi.org/10.1073/pnas.0709704104.
68. **Dargan DJ, Douglas E, Cunningham C, Jamieson F, Stanton RJ, Baluchova K, McSharry BP, Tomasec P, Emery VC, Percivalle E, Sarasini A, Gerna G, Wilkinson GW, Davison AJ.** 2010. Sequential mutations associated with adaptation of human cytomegalovirus to growth in cell culture. J. Gen. Virol. **91:**1535–1546. http://dx.doi.org/10.1099/vir.0.018994-0.
69. **Ryckman BJ, Chase MC, Johnson DC.** 2008. HCMV gH/gL/UL128-131 interferes with virus entry into epithelial cells: evidence for cell type-specific receptors. Proc. Natl. Acad. Sci. U. S. A. **105:**14118–14123. http://dx.doi.org/10.1073/pnas.0804365105.
70. **Huber MT, Tomazin R, Wisner T, Boname J, Johnson DC.** 2002. Human cytomegalovirus US7, US8, US9, and US10 are cytoplasmic glycoproteins, not found at cell surfaces, and US9 does not mediate cell-to-cell spread. J. Virol. **76:**5748–5758. http://dx.doi.org/10.1128/JVI.76.11.5748-5758.2002.
71. **Wille PT, Knoche AJ, Nelson JA, Jarvis MA, Johnson DC.** 2010. A human cytomegalovirus gO-null mutant fails to incorporate gH/gL into the virion envelope and is unable to enter fibroblasts and epithelial and endothelial cells. J. Virol. **84:**2585–2596. http://dx.doi.org/10.1128/JVI.02249-09.
72. **Bodaghi B, Slobbe-van Drunen ME, Topilko A, Perret E, Vossen RC, van Dam-Mieras MC, Zipeto D, Virelizier JL, LeHoang P, Bruggeman CA, Michelson S.** 1999. Entry of human cytomegalovirus into retinal pigment epithelial and endothelial cells by endocytosis. Invest. Ophthalmol. Vis. Sci. **40:**2598–2607.
73. **Dunn W, Chou C, Li H, Hai R, Patterson D, Stolc V, Zhu H, Liu F.** 2003. Functional profiling of a human cytomegalovirus genome. Proc. Natl. Acad. Sci. U. S. A. **100:**14223–14228. http://dx.doi.org/10.1073/pnas.2334032100.
74. **Miller MS, Hertel L.** 2009. Onset of human cytomegalovirus replication in fibroblasts requires the presence of an intact vimentin cytoskeleton. J. Virol. **83:**7015–7028. http://dx.doi.org/10.1128/JVI.00398-09.
75. **Sinzger C, Kahl M, Laib K, Klingel K, Rieger P, Plachter B, Jahn G.** 2000. Tropism of human cytomegalovirus for endothelial cells is determined by a post-entry step dependent on efficient translocation to the nucleus. J. Gen. Virol. **81:**3021–3035. http://vir.sgmjournals.org/content/81/12/3021.long.
76. **Clement C, Tiwari V, Scanlan PM, Valyi-Nagy T, Yue BY, Shukla D.** 2006. A novel role for phagocytosis-like uptake in herpes simplex virus entry. J. Cell Biol. **174:**1009–1021. http://dx.doi.org/10.1083/jcb.200509155.
77. **Duffy C, Lavail JH, Tauscher AN, Wills EG, Blaho JA, Baines JD.** 2006. Characterization of a UL49-null mutant: VP22 of herpes simplex virus type 1 facilitates viral spread in cultured cells and the mouse cornea. J. Virol. **80:**8664–8675. http://dx.doi.org/10.1128/JVI.00498-06.
78. **Subramanian RP, Geraghty RJ.** 2007. Herpes simplex virus type 1 mediates fusion through a hemifusion intermediate by sequential activity of glycoproteins D, H, L, and B. Proc. Natl. Acad. Sci. U. S. A. **104:**2903–2908. http://dx.doi.org/10.1073/pnas.0608374104.
79. **Potena L, Holweg CT, Vana ML, Bashyam L, Rajamani J, McCormick AL, Cooke JP, Valantine HA, Mocarski ES.** 2007. Frequent occult infection with cytomegalovirus in cardiac transplant recipients despite antiviral prophylaxis. J. Clin. Microbiol. **45:**1804–1810. http://dx.doi.org/10.1128/JCM.01362-06.
80. **Stenberg RM, Thomsen DR, Stinski MF.** 1984. Structural analysis of the major immediate early gene of human cytomegalovirus. J. Virol. **49:**190–199.
81. **Maul GG.** 2008. Initiation of cytomegalovirus infection at ND10. Curr. Top. Microbiol. Immunol. **325:**117–132. http://dx.doi.org/10.1007/978-3-540-77349-8_7.
82. **Stinski MF, Petrik DT.** 2008. Functional roles of the human cytomegalovirus essential IE86 protein. Curr. Top. Microbiol. Immunol. **325:**133–152. http://dx.doi.org/10.1007/978-3-540-77349-8_8.
83. **Buchkovich NJ, Maguire TG, Alwine JC.** 2010. Role of the endoplasmic reticulum chaperone BiP, SUN domain proteins, and dynein in altering nuclear morphology during human cytomegalovirus infection. J. Virol. **84:**7005–7017. http://dx.doi.org/10.1128/JVI.00719-10.
84. **Camozzi D, Pignatelli S, Valvo C, Lattanzi G, Capanni C, Dal Monte P, Landini MP.** 2008. Remodelling of the nuclear lamina during human cytomegalovirus infection: role of the viral proteins pUL50 and pUL53. J. Gen. Virol. **89:**731–740. http://dx.doi.org/10.1099/vir.0.83377-0.
85. **Milbradt J, Auerochs S, Sticht H, Marschall M.** 2009. Cytomegaloviral proteins that associate with the nuclear lamina: components of a postulated nuclear egress complex. J. Gen. Virol. **90:**579–590. http://dx.doi.org/10.1099/vir.0.005231-0.
86. **Sinzger C.** 2008. Entry route of HCMV into endothelial cells. J. Clin. Virol. **41:**174–179. http://dx.doi.org/10.1016/j.jcv.2007.12.002.
87. **Huber MT, Compton T.** 1999. Intracellular formation and processing of the heterotrimeric gH-gL-gO (gCIII) glycoprotein envelope complex of human cytomegalovirus. J. Virol. **73:**3886–3892.
88. **Compton T, Nepomuceno RR, Nowlin DM.** 1992. Human cytomegalovirus penetrates host cells by pH-independent fusion at the cell surface. Virology **191:**387–395. http://dx.doi.org/10.1016/0042-6822(92)90200-9.
89. **Smith JD, de Harven E.** 1974. Herpes simplex virus and human cyto-

megalovirus replication in WI-38 cells. II. An ultrastructural study of viral penetration. J. Virol. **14:**945–956.
90. **Sparber F, Tripp CH, Hermann M, Romani N, Stoitzner P.** 2010. Langerhans cells and dermal dendritic cells capture protein antigens in the skin: possible targets for vaccination through the skin. Immunobiology **215:**770–779. http://dx.doi.org/10.1016/j.imbio.2010.05.014.
91. **Sallusto F, Cella M, Danieli C, Lanzavecchia A.** 1995. Dendritic cells use macropinocytosis and the mannose receptor to concentrate macromolecules in the major histocompatibility complex class II compartment: downregulation by cytokines and bacterial products. J. Exp. Med. **182:**389–400. http://dx.doi.org/10.1084/jem.182.2.389.
92. **Trombetta ES, Mellman I.** 2005. Cell biology of antigen processing in vitro and in vivo. Annu. Rev. Immunol. **23:**975–1028. http://dx.doi.org/10.1146/annurev.immunol.22.012703.104538.
93. **Sinclair JH, Baillie J, Bryant LA, Taylor-Wiedeman JA, Sissons JG.** 1992. Repression of human cytomegalovirus major immediate early gene expression in a monocytic cell line. J. Gen. Virol. **73**(Pt 2)**:**433–435. http://dx.doi.org/10.1099/0022-1317-73-2-433.
94. **Huang TH, Oka T, Asai T, Okada T, Merrills BW, Gertson PN, Whitson RH, Itakura K.** 1996. Repression by a differentiation-specific factor of the human cytomegalovirus enhancer. Nucleic Acids Res. **24:**1695–1701. http://dx.doi.org/10.1093/nar/24.9.1695.
95. **Sinclair J, Sissons P.** 2006. Latency and reactivation of human cytomegalovirus. J. Gen. Virol. **87:**1763–1779. http://dx.doi.org/10.1099/vir.0.81891-0.
96. **Saffert RT, Penkert RR, Kalejta RF.** 2010. Cellular and viral control over the initial events of human cytomegalovirus experimental latency in $CD34^+$ cells. J. Virol. **84:**5594–5604. http://dx.doi.org/10.1128/JVI.00348-10.
97. **Woodhall DL, Groves IJ, Reeves MB, Wilkinson G, Sinclair JH.** 2006. Human Daxx-mediated repression of human cytomegalovirus gene expression correlates with a repressive chromatin structure around the major immediate early promoter. J. Biol. Chem. **281:**37652–37660. http://dx.doi.org/10.1074/jbc.M604273200.
98. **Lukashchuk V, McFarlane S, Everett RD, Preston CM.** 2008. Human cytomegalovirus protein pp71 displaces the chromatin-associated factor ATRX from nuclear domain 10 at early stages of infection. J. Virol. **82:**12543–12554. http://dx.doi.org/10.1128/JVI.01215-08.
99. **Hwang J, Kalejta RF.** 2007. Proteasome-dependent, ubiquitin-independent degradation of Daxx by the viral pp71 protein in human cytomegalovirus-infected cells. Virology **367:**334–338. http://dx.doi.org/10.1016/j.virol.2007.05.037.
100. **Tavalai N, Stamminger T.** 2011. Intrinsic cellular defense mechanisms targeting human cytomegalovirus. Virus Res. **157:**128–133. http://dx.doi.org/10.1016/j.virusres.2010.10.002.
101. **Ahn JH, Hayward GS.** 1997. The major immediate-early proteins IE1 and IE2 of human cytomegalovirus colocalize with and disrupt PML-associated nuclear bodies at very early times in infected permissive cells. J. Virol. **71:**4599–4613.
102. **Korioth F, Maul GG, Plachter B, Stamminger T, Frey J.** 1996. The nuclear domain 10 (ND10) is disrupted by the human cytomegalovirus gene product IE1. Exp. Cell Res. **229:**155–158. http://dx.doi.org/10.1006/excr.1996.0353.
103. **Wilkinson GW, Kelly C, Sinclair JH, Rickards C.** 1998. Disruption of PML-associated nuclear bodies mediated by the human cytomegalovirus major immediate early gene product. J. Gen. Virol. **79**(Pt 5)**:**1233–1245.
104. **Nevels M, Paulus C, Shenk T.** 2004. Human cytomegalovirus immediate-early 1 protein facilitates viral replication by antagonizing histone deacetylation. Proc. Natl. Acad. Sci. U. S. A. **101:**17234–17239. http://dx.doi.org/10.1073/pnas.0407933101.
105. **Park JJ, Kim YE, Pham HT, Kim ET, Chung YH, Ahn JH.** 2007. Functional interaction of the human cytomegalovirus IE2 protein with histone deacetylase 2 in infected human fibroblasts. J. Gen. Virol. **88:**3214–3223. http://dx.doi.org/10.1099/vir.0.83171-0.
106. **Groves IJ, Sinclair JH.** 2007. Knockdown of hDaxx in normally non-permissive undifferentiated cells does not permit human cytomegalovirus immediate-early gene expression. J. Gen. Virol. **88:**2935–2940. http://dx.doi.org/10.1099/vir.0.83019-0.
107. **Yuan J, Liu X, Wu AW, McGonagill PW, Keller MJ, Galle CS, Meier JL.** 2009. Breaking human cytomegalovirus major immediate-early gene silence by vasoactive intestinal peptide stimulation of the protein kinase A-CREB-TORC2 signaling cascade in human pluripotent embryonal NTera2 cells. J. Virol. **83:**6391–6403. http://dx.doi.org/10.1128/JVI.00061-09.
108. **Reeves M, Sinclair J.** 2008. Aspects of human cytomegalovirus latency and reactivation. Curr. Top. Microbiol. Immunol. **325:**297–313. http://dx.doi.org/10.1007/978-3-540-77349-8_17.